See related commentary on pg 1055

Nanoparticle-Based Targeting of Vaccine Compounds to Skin Antigen-Presenting Cells By Hair Follicles and their Transport in Mice

Brice Mahe[1,2,5], Annika Vogt[3,5], Christelle Liard[1,2], Darragh Duffy[1,2], Valérie Abadie[1,2], Olivia Bonduelle[1,2], Alexandre Boissonnas[1,2], Wolfram Sterry[3], Bernard Verrier[4], Ulrike Blume-Peytavi[3] and Behazine Combadiere[1,2]

Particle-based drug delivery systems target active compounds to the hair follicle and may result in a better penetration and higher efficiency of compound uptake by skin resident cells. As previously proposed, such delivery systems could be important tools for vaccine delivery. In this study, we investigated the penetration of solid fluorescent 40 or 200 nm polystyrene nanoparticles (NPs) as well as virus particles in murine skin to further investigate the efficacy of transcutaneously (TC) applied particulate vaccine delivery route. We demonstrated that 40 and 200 nm NPs and modified vaccinia Ankara (MVA) expressing the green-fluorescent protein penetrated deeply into hair follicles and were internalized by perifollicular antigen-presenting cells (APCs). Fibered-based confocal microscopy analyses allowed visualizing *in vivo* particle penetration along the follicular duct, diffusion into the surrounding tissue, uptake by APCs and transport to the draining lymph nodes. The application of small particles, such as ovalbumin coding DNA or MVA, induced both humoral and cellular immune responses. Furthermore, TC applied MVA induced protection against vaccinia virus challenge. Our results strengthen the concept of TC targeting of cutaneous APCs by hair follicles and will contribute to the development of advanced vaccination protocols using NPs or viral vectors.

Journal of Investigative Dermatology (2009) **129,** 1156–1164; doi:10.1038/jid.2008.356; published online 4 December 2008

INTRODUCTION

Vaccines have generated major successes in the control of infectious diseases, but several obstacles remain in their development against pandemic chronic diseases, such as HIV, hepatitis C or against cancer. Numerous concepts have successfully been developed in animal models and subsequently been brought to clinical trials. The overall outcome, however, has not met the expectation and is still challenging the field of immunology and vaccine design. Promising approaches for innovation include modifications of the mode of vaccine applications (for example, mucosal, cutaneous), better targeting of high numbers of antigen-presenting cells (APCs) and mechanisms of improved antigen processing and presentation.

Among the various approaches, two different strategies have gained interest during the past years: skin applied vaccine and nanoparticle (NP) compounds (reviewed in Combadiere and Mahe, 2008). The great potential of skin APC targeting is further supported by the finding that the intradermal injection of one-fifth of the dose of a conventional influenza vaccine is sufficient to induce better or equal immune responses than conventional intramuscular (IM) vaccinations (Kenney *et al.*, 2004). Glenn *et al.* (2000) elegantly demonstrated that transcutaneous (TC) vaccine application is safe and efficient. His pioneer studies were followed within the past few years, by different methods for TC immunization such as depilation cream (Shi *et al.*, 1999), abrasion (Guebre-Xabier *et al.*, 2004), or shaving (Glenn *et al.*, 1998a, b). However, those methods are to some extent invasive, require the treatment of large skin surfaces and promote a random penetration through the skin. The small amount of compound, which passes the horny layer, penetrates through the layer of keratinocytes, which are known to be weak immunostimulatory cells (Gaspari and

[1]*Laboratoire d'Immunologie Cellulaire, INSERM U543, Université Pierre et Marie Curie-Paris6, 91 boulevard de l'hôpital, Paris, France;* [2]*Université Pierre et Marie Curie-Paris6, 91 boulevard de l'hôpital, Paris, France;* [3]*Clinical Research Center for Hair and Skin Science, Department of Dermatology and Allergy, Charite—Universitaetsmedizin Berlin, Berlin, Germany and* [4]*Institut de Biologie et Chimie des Protéines, UMR 5086 CNRS/UCBL, 7 Passage du Vercors 69367, Lyon Cedex, France*

[5]*These authors contributed equally to this work.*

Correspondence: Dr Behazine Combadière, Laboratoire d'Immunologie Cellulaire, INSERM U543, Université Pierre et Marie Curie-Paris6, 91 boulevard de l'hôpital, 75013 Paris, France.
E-mail: behazine.combadiere@upmc.fr

Abbreviations: APC, antigen-presenting cell; CFSE, carboxyfluorescein succinimidyl ester; CSSS, cyanoacrylate skin surface stripping; CT, cholera toxin; DC, dendritic cell; DLN, draining lymph node; eGFP, enhanced green-fluorescent protein; FCM, fibered-based confocal microscopy; IM, intramuscular; LC, Langerhans cell; MVA, modified-vaccinia Ankara virus; NP, nanoparticle; OVA, ovalbumin; PBS, phosphate-buffered saline; PFU, plaque-forming unit; TC, transcutaneous; VV, vaccinia virus

Received 2 April 2008; revised 19 July 2008; accepted 10 August 2008; published online 4 December 2008

Katz, 1988). Keratinocyte uptake decreases the antigenic load available for the actual immunization. It is thus crucial to further explore the potential of TC vaccination concepts. Interestingly, Fan *et al.* (1999) found that topical vaccination requires intact hair follicles, pointing to the operation of efficient mechanisms for induction of immune responses to proteins encountered within the follicle. Having been previously identified as a portal for both protein and DNA entry to the skin (Li and Hoffman, 1995), hair follicles are candidates for targeted delivery of therapeutic agents (Lauer *et al.*, 1995).

NP-based vaccine preparations may allow an improved targeting of APCs in the skin compared to nonparticulate systems. This hypothesis is supported by former studies, which suggested that adsorption of vaccine compounds to NPs trigger the activation of APCs and improve their antigen-presenting capacity resulting in better immune responses (Scheicher *et al.*, 1995; Shen *et al.*, 1997; Macklin *et al.*, 1998). In our previous study on human skin explants pretreated with cyanoacrylate skin surface stripping (CSSS), we showed that solid 40 nm NPs penetrated by human hair follicles into the perifollicular tissue, and we isolated NP-positive epidermal Langerhans cells (LCs; Vogt *et al.*, 2006). We used our expertise on particle penetration in human skin to develop a new vaccine application protocol designed to target influenza vaccine into human hair follicles. In a pilot study, we were able to show, that this method was safe and efficient in the induction of cellular immune responses in human volunteers (Vogt *et al.*, 2008). Similarly, Yagi *et al.* (2006) induced cellular immune responses against HIV and melanoma peptides in human volunteers using CSSS technique. Both studies emphasize that the optimization of TC vaccination protocols may allow utilisation of the recently described function of skin LCs as potent inducers of cellular immune responses, to develop new immunization systems, which may be especially valuable for therapeutic vaccination approaches, for example, immunizations against chronic viral diseases or cancer (Ueno *et al.*, 2004; Cao *et al.*, 2007).

The aim of this study was to assess the potential of the hair follicle pathway as a suitable route for vaccine penetration for NPs, protein, DNA, and virus and its efficacy to generate protective immune responses. We investigated the percutaneous penetration, the cellular uptake and the trafficking of 40 and 200 nm solid polystyrene NPs as well as modified vaccinia Ankara expressing the green-fluorescent protein (MVA-eGFP) particles in C57Bl6 mice using *in vivo* fibered-based confocal microscopy (FCM), fluorescence microscopy on cryosections and cell separation techniques. The immunogenicity of model antigens, including ovalbumin (OVA) expressing plasmid and MVA-eGFP particles, was assessed by immune assays to validate our concept of TC targeting of skin APCs with particle-based vaccines.

RESULTS

Penetration of 40 and 200 nm fluorescent polystyrene particles in murine hair follicles surrounded by APCs

To determine the size of particles that can penetrate into the hair follicles, we applied 40 or 200 nm particles on the top of tape-stripped skin on the flank of C57BL/6 mice. The surface area of application was $0.5 \times 0.5\,cm^2$ (Figure 1). The penetration of both 40 and 200 nm NP into the hair follicles was analyzed on longitudinal 5 µm cryosections of the skin, where the fluorescent signal of particles was clearly confined to hair follicle openings (Figure 1, upper panels). Immunofluorescence with anti-CD205 antibodies confirmed that the

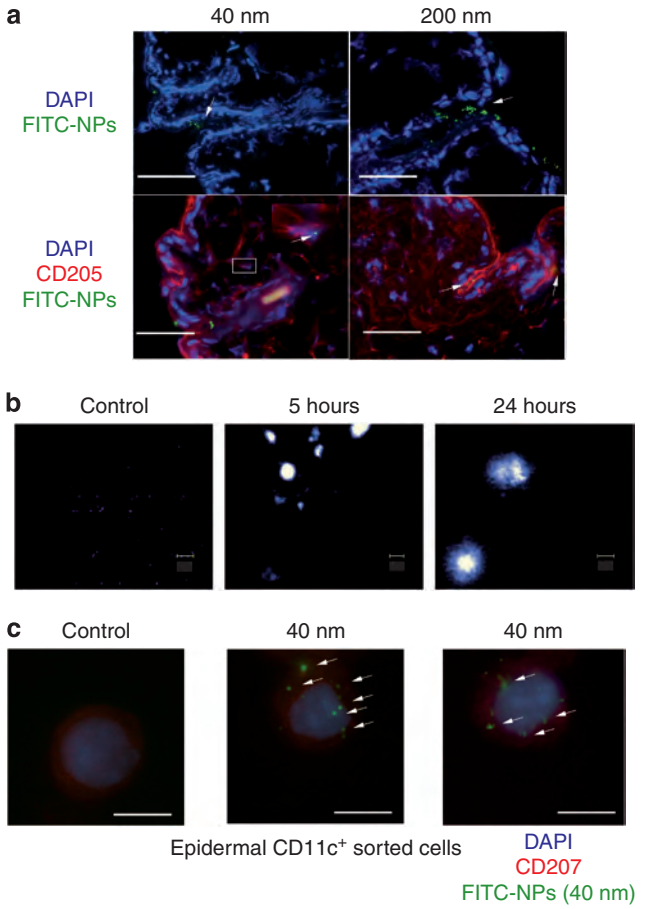

Figure 1. NPs (40 and 200 nm) penetrate into the hair follicles that are surrounded by LCs. (**a**) Four hours following topical application of 2.5×10^{12} fluorescent FITC-NPs (40 and 200 nm, indicated by arrows) on tape-stripped skin flank, analysis of skin cryosections (5 µm thick) revealed aggregation of NPs in the hair follicle openings and penetration along the follicular duct (upper panel). Uptake by dermal DCs was confirmed by immunostaining with anti-CD205 (Texas Red; lower panel). The insert in the lower panel represents a CD205 expressing DC with its expanded dendrites containing 40 nm FITC-labeled NPs). Representative sections are shown. Experiments were performed two times. Bar = 42.5 µm. (**b**) *In vivo* penetration of 40 nm FITC-NPs on tape-stripped skin flank was studied using fibered confocal laser scanning microscopy (FCFM). Well-defined signals of fluorescence with a round shape were obtained at a depth of 80 µm (probe HD-1800) from the skin surface 5 hours after NP application, which correspond to hair follicles. After 24 hours, the signal became diffuse suggesting translocation of 40 nm FITC-NPs into the perifollicular tissue (arrows). Bar = 14 µm (right and left panel) and bar = 12 µm (middle panel). (**c**) To confirm NP uptake by skin APCs, epidermal sheets of flank skin obtained from mice pretreated with 2.5×10^{12} fluorescent 40 nm FITC-NPs were separated, and CD11c+ cells were purified. Microscopic analysis revealed FITC-NPs in CD11c+ CD207 expressing DCs. Bar = 5 µm.

upper part of the hair follicle is especially rich in skin APCs such as dermal dendritic cells (DCs; CD205; (Figure 1, lower panels) and LCs (CD207; data not shown). As shown in Figure 1 (lower panels), dermal DCs containing FITC-NPs (Figure 1a, inset) were localized around the hair follicles and distributed throughout the dermis providing first evidence of NP penetration into the viable tissue.

In vivo investigation of the distribution of topically applied NPs on the skin surface became possible by the use of FCM (Cell-viZio; Mauna Kea Technologies, Paris, France), which allows for *in vivo* confocal microscopy at a depth of 80 ± 5 µm from the skin surface. (Figure 1b). The percutaneous penetration of fluorescent 40 nm NPs was monitored at 5 and 24 hours after topical NP application and compared to control mice. At a depth of 80 µm (maximum depth of Cell-viZio HD-1800 probe) from the skin surface, we found sharp fluorescent signals with round shape (Figure 1b, middle panel). At this depth, the signals correspond to hair follicles filled with fluorescence, that is, they do not reflect surface distribution of fluorescence on the skin. The sharp border of those signals corresponds to the epithelium and the fibrous sheath, which surround the follicular duct. After 24 hours, the fluorescent signal became more diffuse suggesting a translocation of particles in the perifollicular tissue (Figure 1b, right panel as indicated by the arrow).

To determine the nature of APCs that were capable to uptake NPs, we purified CD11c+ cells from the epidermis 3 hours after NPs (40 nm) application. Fluorescent microscopic analysis of individual cells revealed that among CD207+ cells (80% purified CD11c+ cells from the epidermis), 36% contained one or more than one fluorescent particle (Figure 1c, arrows). Our data demonstrate for the first time under *in vivo* conditions, that NPs penetrate into open hair follicles and diffuse into the perifollicular tissue, where they are taken up by epidermal and dermal DCs.

Trafficking of NPs from skin to DLN but not to non-draining lymph nodes

To investigate further distribution and trafficking of fluorescent NPs after hair follicle penetration, we performed FCM on skin draining lymph nodes (DLN) compared to non-DLN at 4, 24, and 48 hours after application of fluorescent NP on tape-stripped skin. As displayed in Figure 2a, FCM showed aggregations of fluorescent particles as early as 4 hours on DLN but not in non-DLN. (Figure 2a and b).

We quantified this migration process from the skin to lymph nodes (LNs) by counting the number of fluorescent spots per field (three mice, 10 fields per LN per mice). Average spots per fields are depicted in Figure 2b. In mice treated with 40 nm particles, the number of fluorescent spots reached a maximum after 24 hours, whereas no signal was detectable in non-DLN (Figure 2b). As shown in Figure 2c, CD11c+ cells purified from DLN contained FITC-NPs. Fluorescent signals within inguinal LNs of mice treated with 200 nm particles were also clearly detectable, albeit less frequently than in mice treated with 40 nm particles, suggesting that the penetration and transport might be less efficient for 200 nm compared to 40 nm NPs.

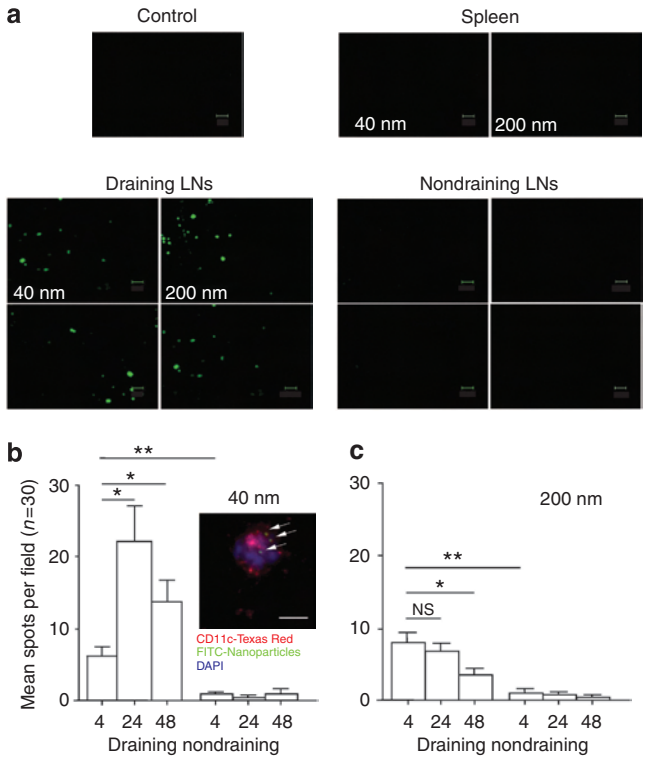

Figure 2. FITC (40 and 200 nm) NPs applied on tape-stripped mouse skin reach the proximal draining lymph nodes. (**a**) Twenty-four hours following topical application of 2.5×10^{12} fluorescent FITC-NPs (40 or 200 nm, respectively) on tape-stripped skin flank, draining lymph nodes, non-DLN and spleen were analyzed by fibered confocal fluorescence microscopy (FCFM), using the surface probe S-1500 (slice thickness of 15 µm and a lateral resolution of 5 µm). Representative fields are shown for each organ and for each size of fluorescent beads. Bar = 32 µm. (**b**) $FITC^+$ spots were counted in 10 randomly photographed fields (three mice per group, total of 30 fields). The mean number of $FITC^+$ spots per field in each organ is shown for 40 nm NPs (left panel) and for 200 nm NPs (right panel) at 4, 24, and 48 hours following application as indicated. Experiments were performed on three mice, twice. Student's *t*-test: $*P<0.05$, $**P<0.01$. Bar = 32 µm. (**c**) Skin draining lymph node cells from 10 mice were isolated and purified with CD11c beads after topical application of 40 nm FITC-NPs on tape-stripped skin flank. At 24 hours, fluorescent 40 nm particles (arrows) were observed in CD11c+ cells. Bar = 32 µm.

Immune response after topical application of ovalbumin DNA plasmid or protein

To test the capacity of antigenic compounds to generate both cellular and humoral responses, 100 µg of plasmid DNA encoding for OVA or 100 µg of ovalbumin protein (pOVA), were applied TC on the flank of tape-stripped mice. In the first set of experiments shown in Figure 3a, we assessed the T-cell responses after adoptive transfer of carboxyfluorescein succinimidyl ester (CFSE)-labeled OT-1 CD8 cells from transgenic mice. We used both CFSE labeling and a congenic CD45.2 marker to follow *in vivo* the behavior of transferred CD8 T cells. Representative dot plots showing $CD8^+CFSE^+$ cells gated on $CD8^+CD45.2^+$ cells at day 4 after vaccination are displayed in Figure 3a. At day 4 after vaccination, we found the most pronounced increase of OVA-specific CD8 cell proliferation (less than six divisions as

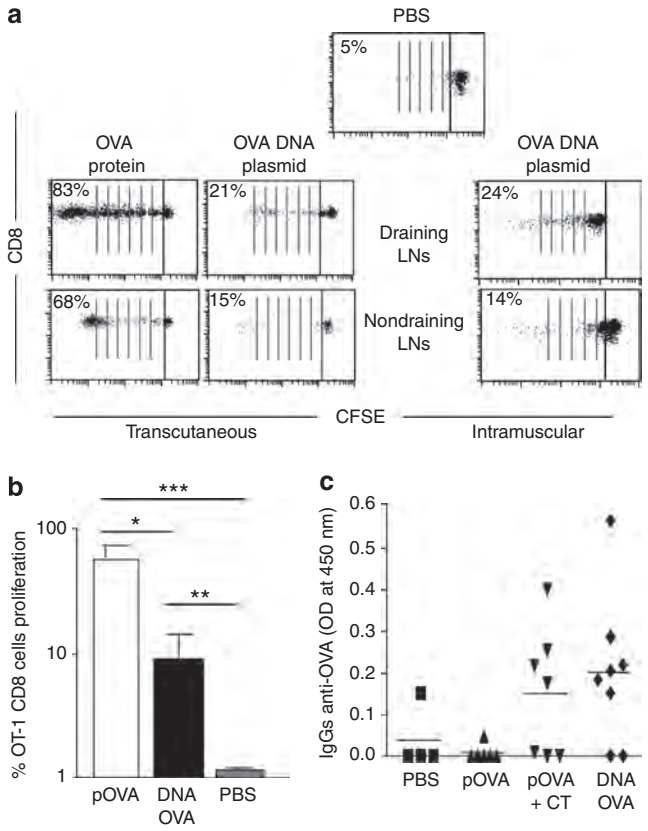

Figure 3. TC application of OVA encoding DNA or OVA protein promotes antigen-specific cellular and humoral responses. (**a**) *In vivo* OVA-specific CD8 T-cell proliferation after TC vaccination. CFSE-labeled OT-1 cells from draining LNs and non-draining LNs were analyzed by flow cytometry. Dot plots represent $CD8^+CFSE^+$ gated on the $CD8^+CD45.2^+$ cells at day 4 after vaccination with 100 μg of OVA DNA plasmid or OVA protein. The percentages of dividing cells are indicated. Results are representative of three different experiments. (**b**) Statistical analysis of the frequency of dividing OT1 cells at day 4 after vaccination with 100 μg of OVA DNA plasmid or OVA protein. Data are representative of three independent experiments. (**c**) Induction of IgGs antibodies against ovalbumin after TC vaccination. Mice were vaccinated with either 100 μg of plasmid DNA coding for ovalbumin (DNA-OVA; $n=8$), OVA protein (pOVA; $n=6$), OVA protein associated with cholera toxin (pOVA + cholera toxin; CT = 10 μg; $n=7$), or PBS ($n=5$). ELISA was performed on peripheral blood mononuclear cells at day 14 after vaccination. Results are representative of three different experiments.

showed by CFSE fluorescent dilution) in DLN proximal to the vaccination site. Cells that have undergone more than six divisions were also found in non-DLN (Figure 3a). These results are in accordance with our previous findings showing that T-cell priming occurs in the DLNs, where antigen is mainly presented and cells, after division and differentiation, migrate to others lymphoid organs (Boissonnas *et al.*, 2004). This was also shown by low numbers of cells in division 1–5 in non-DLN compared to the DLNs. The capacity to induce proliferation was almost nine times higher for protein than for the DNA, which is in accordance with their relatively low immunogenicity shown also after IM immunization (Figure 3b). Overall, both pOVA and DNA-OVA were immunogenic when topically applied after tape stripping. Proliferation of OVA-specific CD8 cells in the LN suggests the transport of the antigen from the skin to the lymphoid organs.

We also monitored the production of specific IgG antibodies after TC application of either pOVA or DNA-OVA by ELISA. In our model, no specific antibodies were detected at day 14 after TC immunization with pOVA compared to control, unless a strong adjuvant such as cholera toxin (CT) was coadministered with the antigen, as previously demonstrated by Glenn *et al.* (1998a) (Figure 3c). DNA plasmid alone, however, induced a humoral response similar to pOVA with CT (Figure 3c) with no significant difference between the two groups ($P>0.05$).

In conclusion, after topical application of OVA coding DNA plasmids or pOVA, cellular immune responses were observed; however, adjuvants might be necessary for a potent induction of humoral immune responses.

Skin penetration and immune response after topical application of modified vaccinia Ankara virus (≈290 nm)

MVA-eGFP encoded particles, with a size of approximately 290 nm, served as a model for particulate antigen (Gallego-Gomez *et al.*, 2003). MVA-eGFP encoded fluorescent virus was used to further investigate the potential of particulate viruses to penetrate the skin and induce cellular and humoral immune responses. Detection of TC applied MVA-eGFP (3×10^7 plaque-forming unit, PFU) in the epidermis was performed using anti-MVA antibodies (Figure 4). Perifollicular diffusion of MVA antigen occurred similar to the results obtained after topical NP application, and we observed the presence of MVA antigen in perifollicular CD207+ cells (Figure 4a). Confocal fluorescent microscopy showed that MVA antigen was detectable particularly in CD207+ cells expanding their dendrites and surrounding the hair follicle as shown by Figure 4b.

To track MVA-eGFP, *in vivo* analysis of fluorescent signal by FCM was performed and revealed the presence of fluorescent infected cells or infected cell debris in the DLN as early as 4 hours after application (Figure 5a). The frequency of fluorescent spots (Figure 5b) was similar to the one observed with 200 nm particles and less frequent than those associated with small 40 nm NPs (Figure 2). The signal then significantly decreased at 24 and 48 hours after application suggesting a degradation of the virus. Rapid processing of this non-propagative virus probably also explains the difficulty to detect MVA-GFP antigens on cryosections in the DLN.

To test whether MVA penetration by the hair follicle is immunogenic, we applied MVA (15×10^6 PFU) on the flank of the animal after tape stripping (Figure 6). As depicted in Figure 6a, a marked increase of IFN-γ producing CD4 and CD8 number was observed demonstrating the induction of a strong cellular response at day 14 after TC immunization. We also observed that CD4 (both IFN-γ^+, IL-2^+) and CD8 (predominantly IFN-γ^+) responded to the MVA stimulation in vaccinated animals. Sera of MVA vaccinated animals by TC route were collected at different time points. As shown in Figure 6b, at day 28, MVA vaccinated animals produced significantly higher level of neutralizing Abs than control group. Mice were then challenged by intranasal route with a

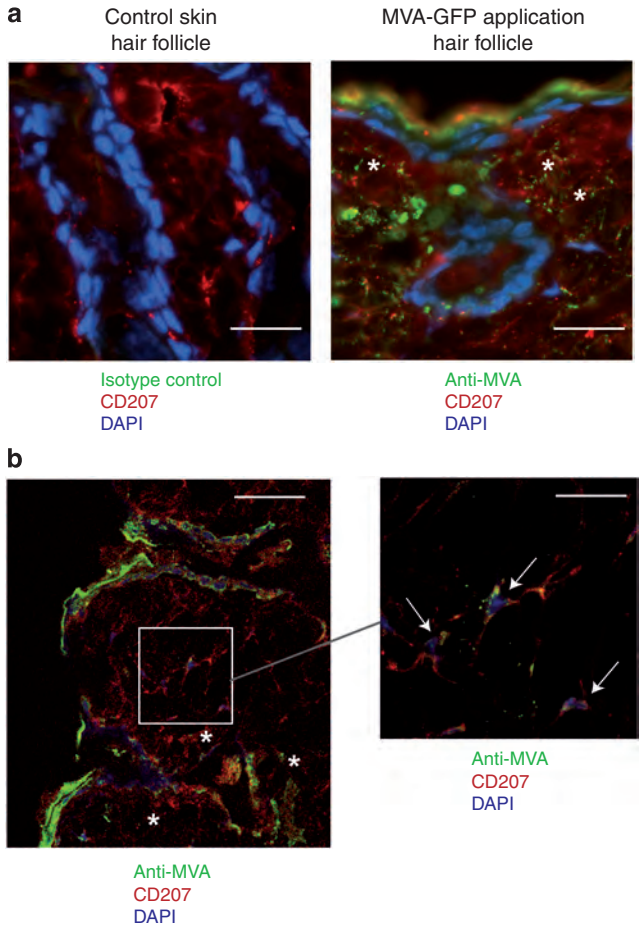

Figure 4. Modified vaccinia Ankara particles (≈290 nm particles) penetrate into tape-stripped skin and are uptaken by antigen-presenting cells. Four hours following topical application of MVA-eGFP on tape-stripped skin flank, skin samples were removed and frozen. Skin cryosections (5 µm thick) were immunostained with antibodies directed against CD207 (Texas Red) expressed on Langerhans cells (LCs) and some DDCs (identification of a new population of langerin+ cells, Bursh, JEM 2007) and anti-MVA (Alexa 488, green). (**a**) MVA-eGFP was detected in TC treated skin (right panel, star) compared to isotype control (left panel). Bar = 189 µm. (**b**) Confocal microscopic analysis (×63, NA 1.4) of CD207+ cells containing MVA-eGFP (indicated by arrows). A network of CD207+ cells expressing MVA antigens can be observed in epidermis and dermis layers surrounding empty follicular ducts. Bar = 51.2 µm (left panel) and bar = 14.2 µm (right panel).

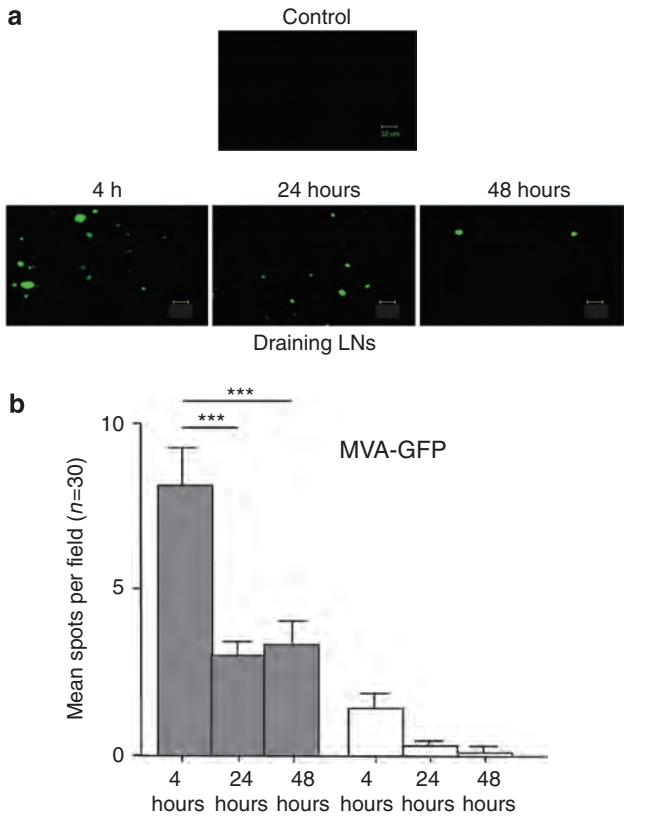

Figure 5. Modified vaccinia Ankara particles (≈290 nm particles) penetrate into the skin and is transported toward the DLN after skin application. (**a**) At different time points following TC application of rMVA-eGFP, draining LNs were analyzed by fibered confocal fluorescence microscopy (FCFM), using the surface probe S-1500 (slice thickness of 15 µm and a lateral resolution of 5 µm). Representative fields for each time point analyzed are shown. Bar = 32 µm. (**b**) Fluorescent spots were counted in 10 randomly photographed fields per mice (three mice per group, total of 30 fields). The mean number of fluorescent spots per field in each organ is shown 4, 24, and 48 hours following application. Student's *t*-test: ***$P<0.0001$. Results are representative of three different experiments.

high dose of live vaccinia virus (VV) and monitored for weight loss (Figure 6c). MVA TC vaccinated animals presented significantly stable weight compared to unvaccinated controls, which developed up to 10% weight loss. Thus, TC application of MVA was immunogenic and protective against virus challenge.

DISCUSSION

The results presented in this study reinforce the proof-of-concept for TC vaccination by demonstrating for the first time that NPs and particulate model vaccines such as MVA-eGFP are capable of penetrating murine skin pretreated with tape stripping. Advanced *in vivo* and *in vitro* microscopy techniques allowed us to identify the hair follicle as a major penetration pathway. All studied particles (40, 200 nm NP and MVA-eGFP encoding virus) penetrated along the follicular duct, translocated into the perifollicular tissue and were taken up by epidermal and dermal APCs, which migrated to the proximal LN. We further demonstrated the capacity of this TC immunization method to generate immune responses after DNA, protein or virus application. The data obtained in this experimental murine model are complementary to our findings obtained on human explants (Vogt *et al.*, 2006) as well as to our clinical pilot study on TC application of influenza vaccine (Vogt *et al.*, 2008).

The aggregation and deposition in hair follicle openings is a key feature of particulate drug preparations, for example, microspheres, solid and flexible NPs, and liposomes (Lademann *et al.*, 2001, 2007). In fact, Lademann *et al.* recently reported retention of 320 nm NPs in hair follicle openings for up to 10 days in humans using *in vivo* confocal laser scanning microscopy, suggesting that topically applied compounds can be stored in hair follicle openings for prolonged periods of time providing time for intensive interactions with the hair follicle epithelium, which, in the

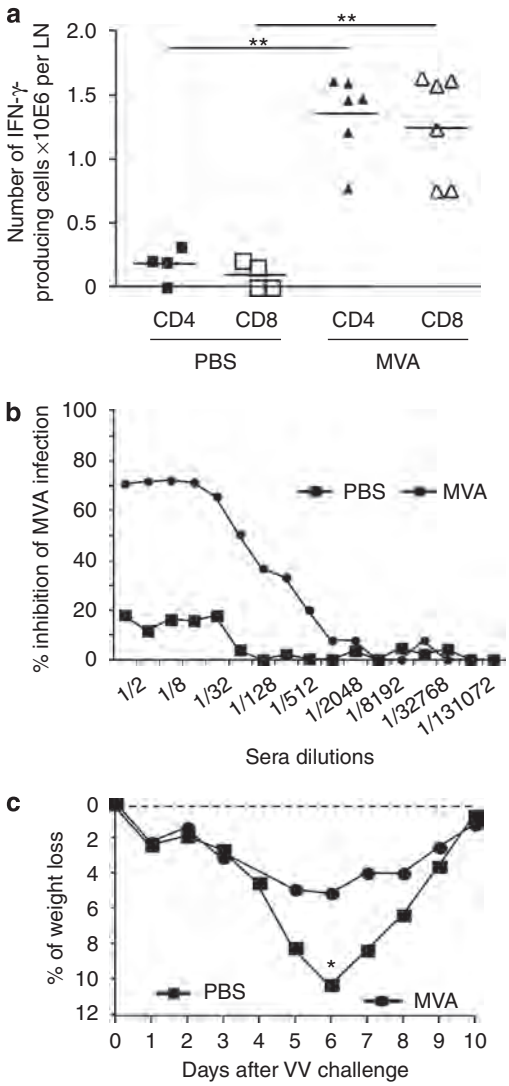

Figure 6. Modified vaccinia Ankara particles based vaccine induces humoral and cellular immune responses by TC route. (**a**) Cytokine production by MVA-specific CD4 and CD8 T cells. C57BL/6 mice received 15×10^6 PFU of MVA, and the CD4 and CD8 T-cell responses in the LN were analyzed on day 14 after application. Lymph nodes were stimulated *in vitro* with 0.1 PFU of MVA per cell for 12 hours. Cells surface were stained with anti-CD4 and anti-CD8, and then cells were stained for intracellular production of IFN-γ. The absolute number of CD4 and CD8 cells producing IFN-γ is indicated per LN. (**b**) Time course of antibody response to TC application of MVA. Results are presented for day 28 posttranscutaneous vaccination. Groups of mice (six per group) received 15×10^6 PFU of MVA or saline buffer as a control. Sera were collected at different time points following immunization and neutralizing antibody titers were determined using the neutralization assay that measures the reduction in infectivity of MVA-eGFP in Hela cells. Results are representative of three different experiments. Differences between PBS and TC immunized groups were analyzed using Mann–Whitney test, $^{**}P<0.01$. (**c**) Protective efficacy of TC immunization with MVA in C57BL/6 mice. Groups of six mice were immunized TC with 5×10^6 PFU of MVA or saline buffer as a control. Two months later, mice were challenged intranasally with 5×10^6 PFU of live vaccinia virus (Copenhagen strain). Individual weight measured daily is presented as a weight loss percentage for both groups. Significant difference in weight loss between control group and TC group is shown, $^{*}P<0.05$.

upper part of the hair follicles, is especially rich in APCs (Christoph *et al.*, 2000).

Although retention of solid particles in the follicular duct has been well documented, there are only a few reports on the penetration of solid particles into the viable tissue. In a study on human skin explants pretreated with CSSS, we recently demonstrated, that solid NPs with a diameter of 40 nm were capable of penetrating human skin after CSSS, which induces mild barrier disruption and opens hair follicles for penetration (Vogt *et al.*, 2006). We confirmed NP uptake by LCs and provided first evidence for the fact that translocation of small NPs into the viable tissue may occur especially in barrier-disrupted skin. On the basis of these observations we concluded that NP-based vaccine preparations might allow improved targeting of APCs in the skin. This hypothesis is supported by former studies, which suggested that adsorption of vaccine compounds to NPs trigger the activation of APCs and improve their antigen-presenting capacity resulting in better immune responses (Scheicher *et al.*, 1995; Shen *et al.*, 1997; Macklin *et al.*, 1998). The results presented in this paper further suggest that small vectors as well as NPs could be used in TC vaccination strategies.

In this study, we further found that the frequency of 40 nm particles found in the DLN was slightly higher than the frequency of 200 nm particles or MVA-eGFP particles suggesting a difference in NP penetration and uptake. This finding is consistent with our previous observations in human skin explants, where the amount and the depth of NP penetration along the follicular duct strongly depends on the size of the particles (Toll, Jacobi *et al.*, 2004). In fact, there is so far little evidence, that NPs at a size exceeding 100 nm penetrate intact skin (Warheit *et al.*, 2007) and inclusion of CSSS into TC vaccination protocols, which aims to target NPs into the viable tissue, is probably crucial. Furthermore, various studies suggest that stripping techniques may not only improve NP penetration, but also exert immunostimulatory effects. It has been shown that the removal of the stratum corneum increased expression of MHC class II, CD86, CD40, CD54, and CD11c on LCs, but did not cause them to migrate (Nishijima *et al.*, 1997; Takigawa *et al.*, 2001). Rapid migration from epidermis to DLN was obtained, however, by exposure to antigen after removal of the stratum corneum, suggesting that maturation and migration of LCs are independently regulated events. Indeed, addition of an adjuvant such as CT increases the immunogenicity of antigen. Similarly, the use of DNA that can activate Toll-like receptors can participate to the maturation of APCs (Dalpke *et al.*, 2002). It has been also shown that the predominant transfected cell types following intradermal or IM inoculations of DNA, however, are keratinocytes after abrasion (Guebre-Xabier *et al.*, 2004). However, the expression of DNA in LCs and DCs remains unknown after TC vaccination. Although the evidence for LCs as the targeted APCs used in topical immunization is indirect, the observations that immunization can be conducted in entirely uninflammed skin and that skin hydration has been involved in this process are highly suggestive that skin penetration and LC targeting occurs. LCs are a specific

subtype of DCs localized in the epidermis. Functional, *in vitro* studies have demonstrated that antigen-pulsed LCs that have been isolated from epidermis can induce T-cell proliferation comparable in magnitude to those induced by similarly pulsed macrophages (Stingl *et al.*, 1978). In addition, MVA application induced an enhanced immune response, which was protective.

In summary, we demonstrated that 40 nm fluorescent polystyrene NPs, after topical application on murine skin, penetrated by hair follicle openings and translocated into the viable tissue, where they were internalized by skin APCs. Moreover, we were able to demonstrate clearly, that within 24 hours, NPs migrated to the proximal LNs, most likely in association with migrating APCs. Further experiments need to be performed to study the process of NP internalization by LCs and DCs and the basis of APC migration and NP transport. The application of small immunogenic compounds such as OVA coding DNA or MVA expressing the eGFP showed that particle-based targeting of hair follicles induced both humoral and cellular immune responses. TC applied MVA induced protection against VV challenge. Further studies using functionalized NPs coated with antigens will help to validate this route of immunization and its use in clinical applications; for example, patch applications of standard vaccines may allow non-invasive large-scale vaccinations, vaccination against chronic viral diseases or cancer. Our data reinforce the concept of TC vaccination with NP-based vaccines. It is an important and highly promising approach for future vaccination strategies (see recent review by our group Combadiere and Mahe, 2008). It takes advantage of two important particle characteristics: improved immunogenicity of particle-bound antigens and preferred penetration by hair follicles, which provide an important interface for NP interactions with the surrounding tissue and APCs and subsequent shuttling to lymphoid tissues.

MATERIALS AND METHODS

Mice

Wild-type C57BL/6 females (6–10 weeks of age) were obtained from Charles River Laboratories (L'arbresle, France). The OT-1 strain is transgenic for the TCR Vα2Vβ5 specific for the peptide OVA257–264 (SIINFEKL), expresses the congenic marker CD45.2 and is restricted to H2-Kb on RAG2−/− background. The OT-1 mice were bred, and all strains were housed at the Nouvelle Animalerie Commune of Pitié-Salpêtrière. All experiments performed at Pitié-salpétrière complied with French legislation and ethics committee guidelines (Departementale des services veterinares).

Antigens

The plasmid vector pVRC2000 used for immunization, coded for the pOVA and its expression was under a human cytomegalovirus promoter (Iga, Boissonnas *et al.*, 2007). DNA were produced by Tebu-Bio (Le Perray en Yveline, France; endotoxin-free, $<30\,\mathrm{EU\,mg^{-1}}$ of DNA). pOVA ($100\,\mu\mathrm{g\,ml^{-1}}$) from chicken egg white (Sigma-Aldrich, St Louis, MO) was diluted in phosphate-buffered saline (PBS) solution before skin administration. Recombinant MVA-eGFP was kindly produced by Dr B Verrier originally provided by Transgene Laboratories (Strasbourg, France). CT was used as an adjuvant (Sigma, France).

Nanoparticles

For all studies, 40 and 200 nm polystyrene particles (FluoreSpheres) were obtained at Molecular Probes, Eugene, OR (yellow–green fluorescent, excitation: 505/515 nm, emission: 515 nm). Storage and handling was performed according to the manufacturer's recommendations. The FluoSpheres particle NeutrAvidin labeled microsphere were supplied as suspensions (1% solids or, respectively) in 50 mM sodium phosphate buffer, 50 mM NaCl, pH 7.5, 0.02% Tween 20 and 5 mM sodium azide. NPs were diluted as indicated before usage. Before sampling, sonication was performed for 1 minute.

Immunofluorescence on frozen tissue sections or fixed cell-suspension analysis

Frozen tissues were cryosectioned (5 μm thick) and sections were fixed for 10 minutes in acetone. Slides were sequentially rehydrated for 10 minutes in PBS, treated for 30 minutes at room temperature with PBS–3% BSA or 0.1% saponin/PBS–3% BSA, and incubated for 1 hour at room temperature with purified rat antimouse CD205 (AbD Serotech, MorphoSys UK Ltd, Oxford, UK) in PBS–BSA 1%, or with biotin rat antiLangerin/CD207 (Euromedex, Souffelweyersheim (67), France) in PBS–BSA 1%, 0.1% saponin. Slides were then incubated 1 hour at room temperature with secondary antibody chicken, respectively, antirat IgG-Alexa fluor 594 or Texas Red-conjugated streptavidin (Invitrogen, Europe, Paisley, UK). For anti-CD207 staining, before antibody staining, endogenous biotin was blocked using the avidin/biotin blocking kit (Vector Laboratories, Burlingame, CA) for 30 minutes at room temperature. After three washes in PBS, slides were mounted with Fluoromount-G (Southern Biotechnology Associates, Birmingham, UK) or Vectashield mounting medium containing DAPI (Vector Laboratories, UK). Slides were analyzed with a fluorescence microscope (BX51; Olympus, Rungis, France) equipped with an image processing and analysis system Qimaging (Media Cybernetics Inc, Silver Spring, MD). For confocal microscopy, we used the Leica Sp2 AOBS confocal microscope from the cell imaging facility of the Pitié Salpétrière, all pictures were taken at $\times 63$, NA 1.4.

In vivo confocal microscopy

In vivo penetration of fluorescent NPs was monitored using noninvasive FCM. The Cell-viZio apparatus (Mauna Kea Technologies) is a fibered confocal fluorescence microscopy imaging system. The two optical probes used for acquisition of the images presented here have respective diameters of 1.5 mm (ref. S-1500-5.0) or 1.8 mm (ref. HD-1800-2.5). The S-1500 probe provides images immediately below the surface of biological tissues, with a slice thickness of 15 μm and a lateral resolution of 5 μm. The HD-1800 probe provides images at 80 μm from the surface with a slice thickness of 20 μm and a lateral resolution of 2.5 μm. During the time of acquisition, mice were anesthetized to avoid any movements. The stripped side of each mouse was wiped with PBS to clean the area prior to acquisition. For the LN study, the organ was skimmed before the surface analysis with the probes. Spots were defined as a unitarian signal presenting a high fluorescent intensity in the center and decreasing levels in the border. At least 10 different areas per organ for at least three mice ($n=30$) were collected and the average numbers of spots per field was calculated. Measurements were performed at different time points as indicated. PBS treated mouse tissues were used for background fluorescence detection.

Transcutaneous immunization

Mice were anesthetized before TC immunization. In absence of any mechanical or chemical treatment, tape-stripping procedures using 10 successive adhesive tapes (Lyréco, France) were applied on the flank of anesthetized C57BL6 mice to remove all the hair and part of the stratum corneum before the topical application of vaccine compounds or NPs as indicated (50 µl on 0.25 cm^2) in 1 × PBS solution (Gibco, Invitrogen cell culture, Europe, Paisley, UK). For each striping, a fresh piece of tape was lightly pressed onto the skin and pulled out. Thus, the surface of treated skin was intact (no irritation seen). The procedure was standardized to avoid highly inflamed or damaged skin. If any of these were observed, mice were excluded from the analysis. Directly after stripping, the solution was applied and allowed to completely air dry and the mice remained anesthetized 1 hour during the procedure avoiding external contacts on the skin. Mice were inspected during the time of experimentation and we did not observe any change in behavior or excessive scratching of the skin.

Intramuscular immunization

Mice were immunized by the IM route (in the anterior tibialis) with 50 µl of either saline solution or 100 µg of plasmid DNA-OVA needle with 26G × $\frac{1}{2}$ inch, 0.45 × 12 mm needle (Terumo Europe, Leuven, Belgium) and 1 ml seringue (BD Plastipak, Becton Dickinson, Madrid, Spain).

Immune responses and cell proliferation

OT-1 CD8 cells, specific for the OVA peptide SIINFEKL (257–264), were isolated from OT-1 transgenic mice LNs, and 4 million CFSE-labeled cells were adoptively transferred by the intravenous route. Naive CD8 T lymphocytes were labeled with 5-(and 6)-CFSE (10 µM; Molecular Probes, Leiden, The Netherlands) as previously described (Boissonnas, Combadiere *et al.*, 2004). Mice were killed 4 days after the transfer for collection of the two inguinal LNs (distal and proximal to the immunized flank) and the spleen. Cell suspensions were prepared as previously described (Boissonnas, Combadiere *et al.*, 2004).

ELISPOT assays

γIFN-ELISPOT kit (Diaclone, Strasbourg, France) was used according to the manufacturer's instruction. Briefly, freshly isolated cells (1.0×10^5 cells) were incubated in triplicates, with or without MVA (0.1 PFU ml^{-1}) or concanavalin A (2.5 µg ml^{-1}). Cells were incubated during 48 hours at 37 °C. Antigen-specific spot-forming cell frequencies were measured on an automated microscope (Zeiss, Munich, Germany) and were counted as positive, if a minimum of 50 spot-forming cell per million peripheral blood mononuclear cells were detected above background.

ELISA

The ELISA was performed by using two 96-well Immulon plates (Dynatech Laboratories, Chantilly, VA); each well was coated overnight at 4 °C with 100 µg of a solution containing either OVA or hen egg white lysozyme (as a control) per well. Specific anti-OVA IgG antibodies were detected after incubation with horseradish peroxidase-conjugated antimouse IgG antibodies (Sigma) diluted in blocking buffer (10% fetal calf serum in PBS) overnight at 4 °C. 3,3,5,5-Tetramethylbenzidine (Sigma) substrate was added. Twenty minutes after, the reaction was stopped with H_2SO_4. Antibody titers were determined by reading the absorbance at 450 nm.

Intracellular cytokine staining

For intracytoplasmic IFN-γ detection, cell suspensions were stimulated overnight with MVA (0.1 PFU per cell) and then incubated for 4 hours at 37 °C with brefeldin A at 5 µg ml^{-1}. The cells were washed and stained with CD4-FITC or CD8α-PercP. After fixation and permeabilization with 1 × PBS–2% fetal calf serum–0.1% saponin, cells were stained with APC-conjugated antimouse IFN-γ and phycoerythrin-conjugated anti-IL-2 antibodies. All antibodies were purchased from BD Biosciences, San Jose, CA. Cells were then run for four-color fluorescence staining on a cytofluorometer (FACS Calibur; BD Biosciences) and 50,000 live events per sample were analyzed with CellQuest software.

Vaccinia virus challenge

Female C57BL/6 mice (6 to 8-week old) were obtained from Charles River Laboratories, and were housed under specific pathogen-free conditions. All experiments complied with local animal experimentation and ethic committee guidelines. For protection studies, mice were immunized with 5×10^6 PFU of MVA by TC route. Two months after immunization, mice were challenged intranasally with 5×10^6 PFU of live VV Copenhagen (generous gift from Transgene Laboratories), and individual body weight was measured daily.

MVA-eGFP neutralization assay

Neutralizing activities were evaluated using an assay based on flow cytometric detection of the GFP (Earl *et al.*, 2003; Cosma, Buhler *et al.*, 2004). This assay used HeLa cells as targets and a recombinant strain of MVA expressing the enhanced Aequoriae GFP (B Verrier). The assay was performed in a 96-well round-bottom tissue culture plate (TPP, Zurich, Switzerland) by adding 2.5×10^4 PFU of MVA-eGFP to 40 µl of serial dilution of heat-inactivated serum in DMEM (Gibco, Invitrogen) supplemented with 2% fetal calf serum (PAA, Laboratories GmbH, Pashing, Austria). The plate was incubated for 1 hour at 37 °C. Then, 1×10^5 HeLa cells were added in 50 µl, and the incubation was carried out for 16 hours in a 37 °C CO_2 incubator. After being washed with PBS supplemented with 0.5% fetal calf serum and 2 mM EDTA, cells were fixed in 2% paraformaldehyde. GFP expression was analyzed on a total of 10,000 events per sample using FACSCalibur and CellQuestPro software (BD Biosciences). The percentage of neutralization was defined as a reduction in the number of GFP-expressing cells compared to the number of GFP-expressing cells in untreated control wells. It was calculated as follows: (1−(percentage of GFP-expressing cells/percentage of GFP-expressing cells in untreated controls)) × 100.

Fluorescent microscopic analysis of isolated epidermal APCs

Briefly, 4 hours after tape stripping and NPs application, the tape-stripped skin from 12 wild-type C57BL/6 females (6–10 weeks of age) was removed and slightly scratched to eliminate the lipid layer. Skins were pooled and incubated for 3 hours in Dispase diluted in RPMI (2.4 U ml^{-1}) at 37 °C. Dermis was then mechanically separated from the epidermis. The epidermis layers were incubated for 15 minutes in 0.05% trypsin-EDTA (Gibco). Single cell solution was obtained by mechanical disruption of tissues on 70 µm Nylon cell-strainer filters (BD Falcon, BD bioscience discovery labware, Redford). The same

procedure was used for NPs detection in epidermis cells but a CD11c+ cell sorting was added before be gently dispersed on Poly-L Lysine coated cover slides (Sigma-Aldrich). Cells were fixed in 2% paraformaldehyde before immunostainning.

CD11c+ cells sorting

Magnetic CD11c+ cell sorting was performed either on LN or skin cells using the CD11c MicroBeads (mouse) and the magnetic-activated cell sorting separation protocol from Miltenyi Biotec, Bergisch, Gladbach, Germany.

Statistical analysis

We used Prism-4 software for data handling, analysis, and graphic representation. Statistical significance was set at $P<0.05$.

CONFLICT OF INTEREST

The authors state no conflict of interest.

ACKNOWLEDGMENTS

This work was supported by ORVACS (Objectifs Recherches VACcins SIDA). B Mahé was supported by a grant from the Ministère de la Recherche et des Technologies. B Combadière is a recipient of Young Investigator Awards of the ''Agence Nationale de Recherche.'' Thanks are also given to the Imaging Cell Facility of the Pitié Salpétrière, for confocal imaging.

REFERENCES

Boissonnas A, Combadiere C, Lavergne E, Maho M, Blanc C, Debré P *et al.* (2004) Antigen distribution drives programmed antitumor CD8 cell migration and determines its efficiency. *J Immunol* 173: 222–9

Cao T, Ueno H, Glaser C, Fay JW, Palucka AK, Banchereau J (2007) Both Langerhans cells and interstitial DC cross-present melanoma antigens and efficiently activate antigen-specific CTL. *Eur J Immunol* 37:2657–67

Christoph T, Muller-Rover S, Audring H, Tobin DJ, Hermes B, Cotsarelis G *et al.* (2000) The human hair follicle immune system: cellular composition and immune privilege. *Br J Dermatol* 142:862–73

Combadiere B, Mahe B (2008) Particle-based vaccines for transcutaneous vaccination. *Comp Immunol Microbiol Infect Dis* 31:293–315

Cosma A, Bühler S, Nagaraj R, Staib C, Hammarin A-L, Wahren B *et al.* (2004) Neutralization assay using a modified vaccinia virus ankara vector expressing the green fluorescent protein is a high-throughput method to monitor the humoral immune response against vaccinia virus. *Clin Diagn Lab Immunol* 11:406–10

Dalpke A, Zimmermann S, Heeg K (2002) CpG DNA in the prevention and treatment of infections. *BioDrugs* 16:419–31

Earl PL, Americo JL, Moss B (2003) Development and use of a vaccinia virus neutralization assay based on flow cytometric detection of green fluorescent protein. *J Virol* 77:10684–8

Fan H, Lin Q, Morrissey GR, Khavari PA (1999) Immunization via hair follicles by topical application of naked DNA to normal skin. *Nat Biotechnol* 17:870–2

Gallego-Gomez JC, Risco C, Rodriguez D, Cabezas P, Guerra S, Carrascosa JL *et al.* (2003) Differences in virus-induced cell morphology and in virus maturation between MVA and other strains (WR, Ankara, and NYCBH) of vaccinia virus in infected human cells. *J Virol* 77:10606–22

Gaspari AA, Katz SI (1988) Induction and functional characterization of class II MHC (Ia) antigens on murine keratinocytes. *J Immunol* 140:2956–63

Glenn GM, Rao M, Matyas GR, Alving CR (1998a) Skin immunization made possible by cholera toxin. *Nature* 391:851

Glenn GM, Scharton-Kersten T, Vassell R, Mallett CP, Hale TL, Alving CR (1998b) Transcutaneous immunization with cholera toxin protects mice against lethal mucosal toxin challenge. *J Immunol* 161:3211–4

Glenn GM, Taylor DN, Li X, Frankel S, Montemarano A, Alving CR (2000) Transcutaneous immunization: a human vaccine delivery strategy using a patch. *Nat Med* 6:1403–6

Guebre-Xabier M, Hammond SA, Ellingsworth LR, Glenn GM (2004) Immunostimulant patch enhances immune responses to influenza virus vaccine in aged mice. *J Virol* 78:7610–8

Iga M, Boissonnas A, Mahé B, Bonduelle O, Combadiére C, Combadiére B (2007) Single CX3CL1-1g DNA administration enhances T cell priming *in vivo*. *Vaccine* 25:4554–63

Kenney RT, Frech SA, Muenz LR, Villar CP, Glenn GM (2004) Dose sparing with intradermal injection of influenza vaccine. *N Engl J Med* 351:2295–301

Lademann J, Otberg N, Richter H, Weigmann HJ, Lindemann U, Schaefer H *et al.* (2001) Investigation of follicular penetration of topically applied substances. *Skin Pharmacol Appl Skin Physiol* 14(Suppl 1):17–22

Lademann J, Richter H, Teichmann A, Otberg N, Blume-Peytavi U, Luengo J *et al.* (2007) Nanoparticles—an efficient carrier for drug delivery into the hair follicles. *Eur J Pharm Biopharm* 66:159–64

Lauer AC, Lieb LM, Ramachandran C, Flynn GL, Weiner ND (1995) Transfollicular drug delivery. *Pharm Res* 12:179–86

Li L, Hoffman RM (1995) The feasibility of targeted selective gene therapy of the hair follicle. *Nat Med* 1:705–6

Macklin MD, McCabe D, McGregor MW, Neumann V, Meyer T, Callan R *et al.* (1998) Immunization of pigs with a particle-mediated DNA vaccine to influenza A virus protects against challenge with homologous virus. *J Virol* 72:1491–6

Nishijima T, Tokura Y, Imokawa G, Seo N, Furukawa F, Takigawa M (1997) Altered permeability and disordered cutaneous immunoregulatory function in mice with acute barrier disruption. *J Invest Dermatol* 109:175–82

Scheicher C, Mehlig M, Dienes HP, Reske K (1995) Uptake of microparticle-adsorbed protein antigen by bone marrow-derived dendritic cells results in up-regulation of interleukin-1α and interleukin-12 p40/p35 and triggers prolonged, efficient antigen presentation. *Eur J Immunol* 25:1566–72

Shen Z, Reznikoff G, Dranoff G, Rock KL (1997) Cloned dendritic cells can present exogenous antigens on both MHC class I and class II molecules. *J Immunol* 158:2723–30

Shi Z, Curiel DT, Tang DC (1999) DNA-based non-invasive vaccination onto the skin. *Vaccine* 17:2136–41

Stingl G, Katz SI, Clement L, Green I, Shevach EM (1978) Immunologic functions of Ia-bearing epidermal Langerhans cells. *J Immunol* 121:2005–13

Takigawa M, Tokura Y, Hashizume H, Yagi H, Seo N (2001) Percutaneous peptide immunization via corneum barrier-disrupted murine skin for experimental tumor immunoprophylaxis. *Ann N Y Acad Sci* 941:139–46

Toll R, Jacobi U, Richter H, Ladermann J, Schaefer H, Blume-Peytavi U (2004) Penetration profile of microspheres in follicular targeting of terminal hair follicles. *J Invest Dermatol* 123:168–76; doi:10.1111/j.0022-202X.2004.22717.x

Ueno H, Tcherepanova I, Reygrobellet O, Laughner E, Ventura C, Palucka AK *et al.* (2004) Dendritic cell subsets generated from CD34+ hematopoietic progenitors can be transfected with mRNA and induce antigen-specific cytotoxic T cell responses. *J Immunol Methods* 285:171–80

Vogt A, Combadiere B, Hadam S, Stieler KM, Lademann J, Schaefer H *et al.* (2006) 40 nm, but not 750 or 1,500 nm, nanoparticles enter epidermal CD1a+ cells after transcutaneous application on human skin. *J Invest Dermatol* 126:1316–22

Vogt A, Mahe B, Costagliola D, Bonduelle O, Hadam S, Schaefer G *et al.* (2008) Transcutaneous anti-influenza vaccination promotes both CD4 and CD8 T cell immune responses in humans. *J Immunol* 180:1482–9

Warheit DB, Borm PJ, Hennes C, Lademann J (2007) Testing strategies to establish the safety of nanomaterials: conclusions of an ECETOC workshop. *Inhal Toxicol* 19:631–43

Yagi H, Hashizume H, Horibe T, Yoshinari Y, Hata M, Ohshima A *et al.* (2006) Induction of therapeutically relevant cytotoxic T lymphocytes in humans by percutaneous peptide immunization. *Cancer Res* 66:10136–44